Intracavity technique for improved Raman/Rayleigh imaging in flames

David F. Marran, Jonathan H. Frank, and Marshall B. Long

Department of Mechanical Engineering and Center for Laser Diagnostics, Yale University, New Haven, Connecticut 06520-8284

Sten H. Stårner and Robert W. Bilger

Department of Mechanical Engineering, The University of Sydney, Sydney, NSW 2006, Australia

A novel intracavity laser diagnostic has been developed to perform quantitative two-dimensional imaging of major species and temperature by using spontaneous Raman scattering and Rayleigh scattering in a turbulent flame. A flash-lamp-pumped dye laser cavity is modified to include sheet-forming optics and 100% reflecting end mirrors. In a comparison of this system with a laser configuration with the sheet-forming optics outside the cavity, the beam waist is comparable, while the intensity is increased by a factor of 5. This technique has applicability to many systems in which weak scattering must be monitored, such as Rayleigh scattering, Raman scattering, and laser-induced fluorescence of certain combustion radicals.

Intracavity laser spectroscopy has long been recognized as an effective way to boost the signal-to-noise ratio of weak molecular scattering or absorption processes. This technique has been demonstrated for a variety of line-of-sight absorption measurements,[1,2] including radical concentration measurements in laminar flames.[2] Intracavity configurations have also been used to enhance the weak signals in single-point Raman scattering studies.[3–5] In combustion diagnostics, however, increased emphasis has been placed on techniques capable of planar measurements. Two-dimensional Raman imaging in turbulent flames has been done successfully by use of a sheet-forming multipass cell, consisting of a pair of cylindrical reflectors located outside the laser cavity.[6–8] Although the multipass cell requires precise alignment, its use results in a significant increase in intensity compared with forming a sheet by use of a single laser pass and conventional cylindrical optics.[8] The main difficulty with the application of the multipass cell to turbulent flames is due to the index of refraction gradients produced by the flame. The beam steering effects of the gradients are amplified over the many passes through the flame, resulting in an increased beam waist, sheet intensity modulations that cannot be corrected, and an increase in elastically-scattered light off the multipass mirrors.[6] In this study we have demonstrated a two-dimensional intracavity imaging technique that has the benefits of increased laser intensity, while minimizing the problems associated with the application of a multipass cell to turbulent flames. As a demonstration of the utility of the approach, the intracavity Raman/Rayleigh imaging technique has been used to determine the mixture fraction distribution in a turbulent nonpremixed flame.

The mixture fraction, ξ, is defined as the mass fraction of all atoms originating in the fuel stream (regardless of their molecular bonding) and is independent of the chemical reaction occurring in the flame. In addition, one needs the gradient of the mixture fraction to find the scalar dissipation, χ, which determines the rate of molecular mixing in the flow ($\chi = 2D|\nabla\xi|^2$, where D is the diffusivity). The mixture fraction and its gradient are important in the modeling of turbulent flames,[9] and the experimental determination of mixture fraction over a wide field is essential for testing these models.

A two-scalar approach for mixture fraction determination that uses single-point Raman and Rayleigh data in a turbulent methane flame was developed by Stårner et al.[10] The method assumes unity Lewis number and a simplified one-step reaction between fuel and oxidizer. It has been shown that the measurement of fuel concentration and Rayleigh scattering is sufficient to determine the mixture fraction. Fuel concentration has been obtained by use of Raman scattering from the fuel[6,11,12] or laser-induced fluorescence of the fuel or fuel marker.[12] The Raman work has shown the most promise because simpler hydrocarbons may be used, reducing the effects of pyrolysis on the fuel measurement.

The experimental setup for intracavity Raman/Rayleigh imaging is shown in Fig. 1. The output coupler from a flash-lamp-pumped dye laser (Candela LFDL-20 with Pyromethene 546 dye, 10-mm-diameter dye cell) is replaced with a cylindrical mirror [7.6-cm focal length (fl)], and the cavity is extended to approximately 2.75 m. An antireflection-coated cylindrical lens (30-cm focal length) is placed within the cavity such that light reflected by the cylindrical mirror is recollimated and fed back into the cavity. (The use of a cylindrical lens without antireflection coating was found to make minimal difference in the sheet intensity, which suggests the possibility of using this approach even in the presence of windows.) Alignment is performed with a pellicle beam splitter that couples the
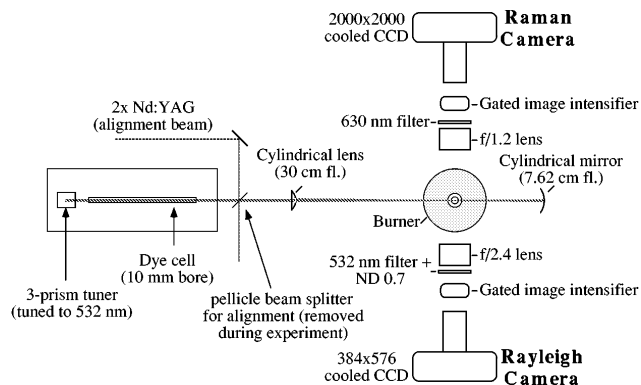
Fig. 1. Experimental configuration for intracavity Raman/Rayleigh imaging.

second harmonic of a Nd:YAG laser (532 nm) into the laser cavity. When alignment is complete the pellicle is removed, and the cavity is fine tuned to optimize the beam profile. The increased feedback from the cylindrical mirror results in significant gains in sheet intensity. Because the cavity mirrors are well away from the region being imaged, the Rayleigh background from surfaces is less than 1.5% of the ambient air signal and is unaffected by the flame. In addition, because the end mirrors are perpendicular to the beam, sheet intensity modulations occur only parallel to the beam, making corrections quite simple.

In order to measure the sheet thickness, we introduced an aerosol of submicrometer-sized water droplets into the illumination sheet. The Lorenz–Mie scattering from the aerosols was imaged onto a CCD camera (SBIG ST-6, with $f/22$ optics to provide a large depth of field) situated above the laser sheet. The waist was measured to be 0.75 mm FWHM. We used spontaneous Raman scattering from nitrogen to estimate the increase in sheet intensity by comparing the signal from the intracavity setup with that obtained from a single pass from a 1.8-m extracavity setup with a 40% output coupler. The intracavity approach provided a signal 5.2 times larger than that obtained with the extracavity setup, which contained 1 J of energy at 532 nm with a 0.75-mm sheet thickness. In order to reduce the intracavity sheet thickness slightly, we placed an 8.5 mm vertical slit within the laser cavity (the bore of the dye cell was 10 mm and determined the sheet height). The slit reduced the beam waist to 0.56 mm and the signal to 4.2 times that obtained with the 1-J extracavity setup. With or without the slit, no thickening of the sheet was found to occur when the beam passed through large refractive-index gradients generated with a helium jet.

The scattered Raman and Rayleigh light was detected with two intensified CCD cameras located on opposite sides of the laser sheet, as shown in Fig. 1. The Raman-scattered light from methane was isolated with an interference filter (630 nm, 10-nm FWHM) and focused onto a single-stage intensifier by an $f/1.2$ camera lens. The output of this intensifier was optically coupled to a cooled CCD detector. The Rayleigh light was collected with an $f/2.4$ camera lens, isolated with an interference filter (532 nm,

10-nm FHWM), and imaged onto a single-stage intensifier. A ND 0.7 filter was added to keep the intensifier within its linear regime. The intensifier was optically coupled to the second CCD. We suppressed flame luminosity by gating the intensifiers around the 3-μs laser pulse. The images obtained were then transferred to a computer for storage and processing.

Once in the computer, the two images were scaled, rotated, and cropped to allow them to be compared on a pixel-by-pixel basis. After this matching, each pixel corresponded to a volume of 0.06 mm $\times$ 0.06 mm $\times$ 0.56 mm, with the largest value corresponding to the sheet thickness. Images were recorded 25 diameters downstream from a 6.1-mm axisymmetric piloted nonpremixed methane–air flame. The burner was placed in a 7-m/s filtered coflow to prevent particles from interfering with the Rayleigh data. Flames with nozzle Reynolds numbers ranging from laminar to 34,800 were investigated with air-diluted methane used as fuel (30% methane by volume). In all cases, no soot interference was observed in the images. The background for the Rayleigh data was obtained with helium in the manner described in Ref. 8. The edge of each Rayleigh image contained a region of ambient air to account for the shot-to-shot fluctuations in the laser profile and energy. The Rayleigh intensity measured in this region was used to correct the laser profile fluctuations in both the Rayleigh and Raman images. This approach works quite well. In a 50-image turbulent flame data set, the rms sheet intensity modulation in the central 8 mm of the ambient-air portion of each image was calculated. On average, the modulation was reduced from 12%
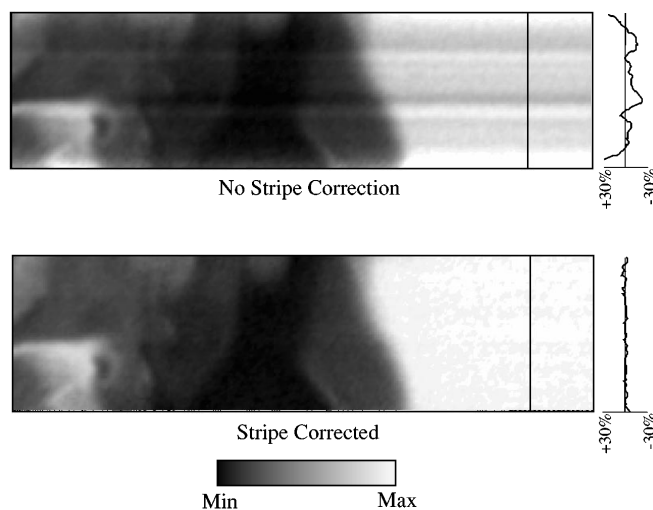

Fig. 2. Stripe correctability of the Rayleigh data from a piloted, turbulent nonpremixed methane–air flame ($Re = 21,300$). The measurements have been taken 25 diameters downstream ($d = 6.1$ mm) and were cropped to 8 mm in the axial by 30 mm in the radial directions. For this image, the rms modulation of the laser across the image is reduced from 17.8% to 1.2% in ambient air. The line plot adjacent to each image corresponds to a slice across the laser beam along the line shown. The Rayleigh intensity is represented by a linear gray scale, with lighter shades corresponding to larger values.
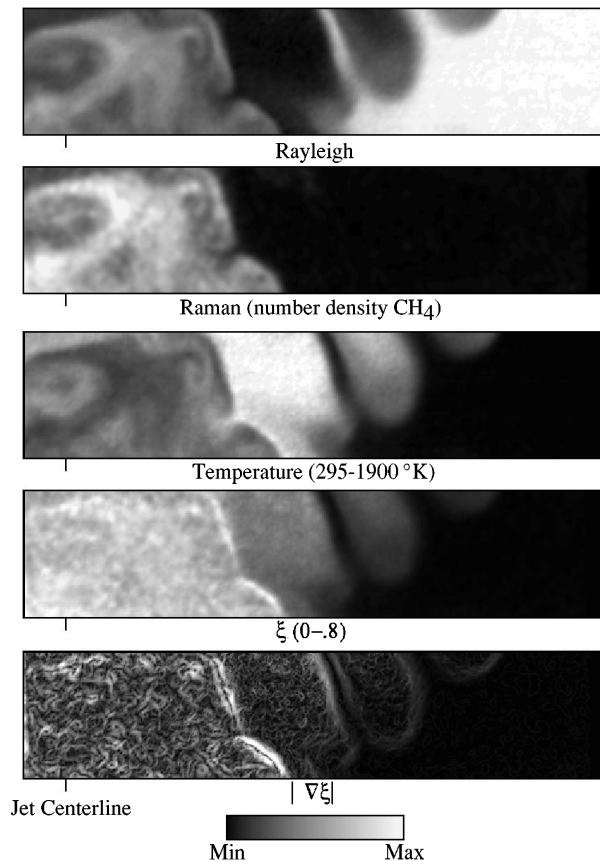
Rayleigh

Raman (number density CH_4)

Temperature (295-1900 °K)

ξ (0–.8)

Jet Centerline $|\nabla\xi|$

Min   Max

Fig. 3. Raman/Rayleigh images from a piloted methane−air flame. The data were taken under the same conditions as in Fig. 2 and were cropped to 6.5 mm in the axial by 30 mm in the radial directions. The Rayleigh image is related to temperature, and the Raman image measures the number density of methane. Also shown are the calculated temperature, mixture fraction (ξ), and magnitude of the mixture fraction gradient ($|\nabla\xi|$) for this image pair. In each image, the scalar value is represented by a linear gray scale, with lighter shades corresponding to larger values.

to less than 0.7% [signal-to-noise ratio (SNR) $\approx$ 80]. Figure 2 shows the Rayleigh data before and after stripe correction. For the Raman image, the SNR across the beam is 39 for pure methane.

In order to increase the SNR further in the Raman data, smoothing with a Gaussian weight function ($\sigma_x = \sigma_y = 2.3$ pixels, out to $\pm 1.75\sigma$) was applied. This level of smoothing increased the SNR three to five times (the unsmoothed flame data had an average SNR $\approx$ 7). A sample of the corrected Rayleigh/Raman data, along with the temperature, mixture fraction, and magnitude of the mixture fraction gradient, is shown in Fig. 3. The peak temperatures measured are very close to the adiabatic flame temperature for the fuel ($T_{\mathrm{ad}} = 1890$ K). As expected, the mixture fraction is largest in the fuel pockets along the center line of the jet, passes through stoichiometric at the flame front ($\xi_{\mathrm{st}} = 0.287$), and decays to zero in air. The magnitude of the mixture fraction gradient is largest just rich of stoichiometric, indicating zones of intense molecular mixing in this region.

The use of intracavity Raman/Rayleigh scattering has proved to be a significant advance for mixture fraction imaging in turbulent nonpremixed flames. The high sheet intensity available with the intracavity setup makes calculation of the scalar dissipation feasible. In addition to using Raman/Rayleigh imaging, the technique has been modified and shown to work for Raman N_2/Raman CH_4 imaging. Combinations of these two scalars should be sufficient to determine the mixture fraction, and because the Raman wavelengths are separated from the laser wavelength, it should be possible to combine particle imaging velocimetry with mixture fraction imaging. Alternatively, the dye laser could be tuned to a wavelength that would permit the imaging of combustion radicals (through fluorescence) with mixture fraction. The intracavity approach has applicability to a variety of circumstances in which two-dimensional imaging of a weak scattering process is necessary. The substantial increase in laser energy, good beam thickness, and excellent correctability of the laser sheet intensity profile provide an excellent framework for future applications.

References

1. F. Stoeckel and G. H. Atkinson, Appl. Opt. **24,** 3591 (1985); R. J. Thrash, H. von Weyssenhoff, and J. S. Shirk, J. Chem. Phys. **55,** 4659 (1971).
2. S. J. Harris, Appl. Opt. **23,** 1311 (1984); S. J. Harris and A. M. Weiner, Opt. Lett. **6,** 434 (1981).
3. P. H. Young and H. W. Latz, Spectrosc. Lett. **16,** 471 (1983).
4. R. A. Hill, A. J. Mulac, and C. E. Hackett, Appl. Opt. **16,** 2004 (1977).
5. A. Weber, S. P. S. Porto, L. E. Cheesman, and J. J. Barret, J. Opt. Soc. Am. **57,** 19 (1967).
6. J. B. Kelman, A. R. Masri, S. H. Stårner, and R. W. Bilger, in *Proceedings of the Twenty-Fifth Symposium (International) on Combustion* (Combustion Institute, Pittsburgh, Pa., 1994).
7. R. W. Schefer, M. Namazian, and J. Kelly, Opt. Lett. **16,** 858 (1991); M. B. Long, P. S. Levin, and D. C. Fourguette, Opt. Lett. **10,** 267 (1985); B. F. Webber, M. B. Long, and R. K. Chang, Appl. Phys. Lett. **35,** 119 (1979).
8. M. B. Long, in *Instrumentation for Flows with Combustion,* A. K. M. P. Taylor, ed. (Academic, London, 1993), p. 467.
9. R. W. Bilger, in *Instrumentation for Flows with Combustion,* A. K. M. P. Taylor, ed. (Academic, London, 1993), p. 1.
10. S. H. Stårner, R. W. Bilger, R. W. Dibble, and R. S. Barlow, Combust. Sci. Tech. **86,** 223 (1992).
11. J. H. Frank, K. M. Lyons, D. F. Marran, M. B. Long, S. H. Stårner, and R. W. Bilger, in *Proceedings of the Twenty-Fifth Symposium (International) on Combustion* (Combustion Institute, Pittsburgh, Pa., 1994).
12. S. H. Stårner, R. W. Bilger, K. M. Lyons, J. H. Frank, and M. B. Long, Combust. Flame **99,** 347 (1994).